



THE 15th CHESAPEAKE SAILING YACHT SYMPOSIUM



International America's Cup Class Yacht Design Using Viscous Flow CFD

Paul Jones, Science Applications International Corporation, Annapolis, MD.

Rich Korpus, (formally of) Science Applications International Corporation, Annapolis, MD.

ABSTRACT

The Computational Fluid Dynamics (CFD) tools needed to incorporate viscous effects into design trade-off studies have finally matured to the point where practical guidance can be provided within design cycle turn-around times. The required techniques are known as Reynolds-Averaged Navier-Stokes (RANS) solvers, and saw their first practical application to yacht design during America's Cup XXX. The team of AmericaOne, for example, utilized RANS for upwind sail design and VPP aerodynamic force predictions. RANS was also used in the keel design process, and to provide "virtual prototyping" for investigating new concepts before building them. This paper presents some of these ground-breaking applications, and demonstrates the types of guidance available to the designer using RANS.

INTRODUCTION

America's Cup racing has long relied on inviscid CFD to guide the development of keel and hull. Americas Cup XXX, however, saw the first application of state-of-the-art viscous flow computational methods. Motivating this change was the fact that hull design methods have matured to a point where nearly optimal boats can be produced for a given speed. Gains in hull performance are getting harder to find, and improvements in sail design are required to maintain the competitive edge. Since many of the trade-offs needed to optimize an IACC rig are effected by viscosity, a totally new design methodology is required.

Such a revolution could be instigated in two ways: experimental testing; and "high-fidelity" computational tools such as Reynolds-Averaged Navier-Stokes (RANS) codes. Each method has its advantages and disadvantages. Wind tunnel data, for example, can provide accurate force data, but contains too much experimental scatter for identifying the smallest design trends. Wind tunnel results can also prove misleading

due to the presence of scale effects. Since viscosity is responsible for much of the drag of an aerodynamic body, inviscid computational techniques such as panel methods cannot always be utilized.

RANS techniques provide a useful alternative to wind tunnel testing. They resolve all the physics of a real flow field, and can therefore accurately predict even the most subtle viscous trends. They can incorporate environmental effects such as the Earth's boundary layer and twist in the apparent wind angle. They can provide full scale predictions, resolve the effects of stall (e.g. aerodynamic separation on the mast or sails), and can capture the subtle relationship between lift and drag as a sail is made fuller or flatter.

The cost of resolving this level of detail is that a numerical model must be built to represent the entire airspace around a boat. This can be quite time consuming, and traditional approaches often require months for geometries as complex as America's Cup Class boats. In order to circumvent this bottleneck a technique known as "overset gridding" is used. The method enables complete automation of the grid generation process, and yields a system limited only by the available computer power. It also insures that all grids are "geosyms," and therefore eliminates solution variability associated with subtle differences between grids. Incorporation of the overset method improved productivity from about one analysis per month to more than 25 per week -- a two order-of-magnitude increase. It also improved accuracy sufficiently to resolve drag differences as small as 1/2%.

It is important to note that RANS fits into the design process not as a replacement to existing design tools, but rather as a supplement for those cases where more detailed trending is required. Similarly, RANS is not intended as a replacement to model testing. While RANS is the best tool for identifying very subtle performance trends, it does not necessarily predict overall forces to the same accuracy level as an

experiment. Nor can it duplicate the quantity of data available from panel codes – an attribute essential to populate a VPP's databases. Experiments and less high-fidelity computational tools (e.g. panel methods) are still an essential part of a complete design process.

APPROACH

The RANS code used for all AmericaOne design analyses is the Finite-Analytic Navier-Stokes (FANS) software package. FANS is an unsteady, incompressible, three-dimensional RANS solver with extensive validation on a wide range of high-Reynolds number steady and unsteady flows (e.g. Korpus et. al. 2000, 1998, Kumarasamy and Korpus 1997, Weems, et. al., 1994, Chen et. al. 1991). It solves the Reynolds-averaged form of the Navier-Stokes equations

When non-dimensionalized by a characteristic length L , velocity V_0 , and density ρ , the Cartesian form of these governing equations can be written

$$\nabla \cdot \mathbf{V} = 0 \quad (1)$$

$$\frac{\partial \mathbf{V}}{\partial t} + \mathbf{V} \cdot \nabla \mathbf{V} + \nabla p - \frac{1}{\text{Re}} \nabla^2 \mathbf{V} - \nabla \cdot \boldsymbol{\tau} = \mathbf{F} \quad (2)$$

$$\frac{\partial k}{\partial t} + \mathbf{V} \cdot \nabla k - \left(\frac{1}{\text{Re}} + \nu_t \right) \nabla^2 k - P + \varepsilon = 0 \quad (3)$$

$$\begin{aligned} \frac{\partial \varepsilon}{\partial t} + \mathbf{V} \cdot \nabla \varepsilon - \left(\frac{1}{\text{Re}} + \frac{\nu_t}{1.3} \right) \nabla^2 \varepsilon - \frac{\varepsilon}{k} (c_{\varepsilon 1} P_{sol} + c_{\varepsilon 3} P_{irr}) \\ + c_{\varepsilon 2} \frac{\varepsilon^2}{k} = 0 \end{aligned} \quad (4)$$

where the Reynolds stress components τ_{ij} are defined by the Boussinesq approximation.

$$\tau_{ij} \equiv -\frac{2}{3} k \delta_{ij} + \nu_t S_{ij}, \quad S_{ij} = \frac{\partial u(i)}{\partial x^j} + \frac{\partial u(j)}{\partial x^i} \quad (5)$$

and $[x^1, x^2, x^3]^T$ represents the Cartesian position vector. \mathbf{V} represents the Cartesian velocity's vector $[u(1), u(2), u(3)]^T$, p the pressure, k the turbulent kinetic energy, and ε the turbulent dissipation rate. \mathbf{F} is an arbitrary body force used to represent propulsor effects. The quantity ν_t is defined as the linear eddy viscosity $.09 k^2/\varepsilon$, and Re the Reynolds number LV_0/ν . The rate of production of k is represented by P , and production in the ε equation has been split into its solenoidal and irrotational components following Hanjalic and Launder (1980):

$$P = P_{sol} + P_{irr} \quad (6)$$

$$P_{sol} = 4[S_{12}^2 + S_{13}^2 + S_{23}^2] \quad (7)$$

$$P_{irr} = 2[S_{11}^2 + S_{22}^2 + S_{33}^2] \quad (8)$$

The modeling coefficients $C_{\varepsilon 1}$, $C_{\varepsilon 2}$, $C_{\varepsilon 3}$ are taken as constants set equal to (1.44, 1.92, 2.4), respectively.

The usual near-wall stiffness problem associated with Eq.(4) has been circumvented herein by using the two-layer approach of Chen and Patel (1988, 1989). The approach utilizes the $k\varepsilon$ model outlined above for most of the flow field, but a one-equation kl model in the viscous sublayer and buffer zone. Switching between ε and l dissipation models is performed automatically when the wall Reynolds number $\text{Re}_{\text{wall}} = \text{Re} \sqrt{k\delta}$ (δ being the nondimensional distance to the closest wall) becomes less than 300 (Chen and Korpus, 1993). Details of the l dissipation model can be found in Chen and Patel (1989) and will not be repeated here.

Computations about complex geometries requires that Equations (1) through (4) be first transformed into body fitted coordinates. This is accomplished by defining a curvilinear system (ξ^1, ξ^2, ξ^3) such that any physical boundary in the domain coincides with one or more surfaces of constant ξ^i . The system need not necessarily be orthogonal, and can be defined separately for each block of the grid. All independent variables in Equations (1) through (4) are then transformed to (ξ^1, ξ^2, ξ^3) space by chain rule while leaving the dependant variables Cartesian.

With the equations in their curvilinear form, the discretization is accomplished by linearizing each equation, over a computational element, then solving analytically by separation of variables. Evaluation of the analytic solution at the interior node of a computational element provides a stencil for the center point in terms of its nearest neighbors.

Time derivatives are handled by the Euler implicit method, and unknowns from the previous time step are lumped into the source term. The resulting implicit system equations is solved by the alternating direction implicit (ADI) method in each cross-flow plane, and then swept repetitively in the streamwise direction. Detailed expressions for the coefficients of the finite-analytic stencil can be found in Chen et al. (1990).

Pressure coupling is supplied using a modified SIMPLER/PISO algorithm (Chen and Patel, 1989) that uses the strong conservation form of Eq. (1)

$$\frac{\partial \sqrt{g} U^1}{\partial \xi^1} + \frac{\partial \sqrt{g} U^2}{\partial \xi^2} + \frac{\partial \sqrt{g} U^3}{\partial \xi^3} = 0 \quad (9)$$

where U^i is the contravariant velocity $U(1)\partial \xi^1 / \partial x^1 + U(2)\partial \xi^2 / \partial x^1 + U(3)\partial \xi^3 / \partial x^1$ and g is the determinant of the covariant fundamental metric tensor. The technique defines pseudo-velocities from the discretized form of Eq.(2) as:

$$U^i = \hat{U}^i + E^{ii} \frac{\partial p}{\partial \xi^i} \quad (10)$$

where \hat{U}^i and E^{ii} necessarily involve the finite-analytic coefficients, and will not be repeated here (see Chen and Korpus 1993).

A Poisson equation for pressure is then derived by substituting equation (10) into (9), and discretizing using central differences. By centering the differences in equation (10) on staggered grid locations, the resulting Poisson equation involves unknowns only at the grid nodes. The technique is thus unique in that it does not require staggered velocity and pressure variables.

Selected geometries are discretized using a mixture of Earth-fixed Cartesian blocks and body-fitted curvilinear blocks. FANS' moving-grid overset capability is used to join the two, and facilitates relative movement for unsteady and/or structural interaction problems (e.g. membrane sail studies). The method greatly diminishes the user overhead in gridding by permitting the generation of arbitrarily overlapped blocks around complex geometries. The result is better quality grids (and therefore more accurate solutions), with fewer points produced in less time.

Grid generation is performed using the NASA Ames Research Center's HYPGEN suite of codes. The system consists of a series of hyperbolic grid generation utilities that are driven by simple script inputs. Their advantage lies with the fact that they can be used to automate the grid generation process, and have been efficiently coupled to SAIC's RANS code using the overset method. Completely automatic grid generation was achieved during the last America's Cup by taking IGES geometry descriptions from North Sail's CAD system, using HYPGEN to generate grids around each geometry piece (e.g. head stay, mast, mainsail, genoa, and hull), and then using the overset method to initialize the RANS solution. The entire process was driven by a series of UNIX shell scripts, and the scripts set to loop over a given number of design geometries. The resulting system enabled full utilization of a 128-processor HP supercomputer with very little user intervention.

Figure 1 demonstrates the extent to which a typical geometry was detailed (only surface grids are depicted). All attributes important to an accurate flow analysis can be resolved utilizing the strengths of the overset grid. Included in the rig analysis, for example, are the mainsail, Genoa, mast, head stay, hull, deck, cockpit, and Earth's boundary layer.

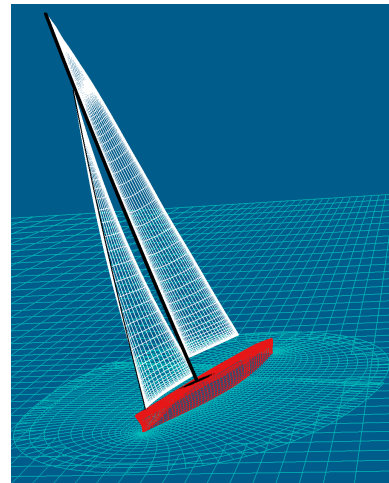


Figure 1: Typical Rig Aerodynamics Grid for Americas Cup Class Yachts

QUALITATIVE FLOW RESULTS

Although CFD is used mainly as a quantitative tool to rank design alternatives, the qualitative data provided can have an equally significant impact on the design process. Alleviation of poor flow attributes, for example, requires that their cause be traced back to the geometry elements that cause them. Figure 2 demonstrates a few examples of how RANS provides such a capability. The figure shows sail load colored by pressure difference, and includes streamlines to highlight the boom and deck-edge vortices. If any of these features indicated a design problem, it's cause could be easily identified.

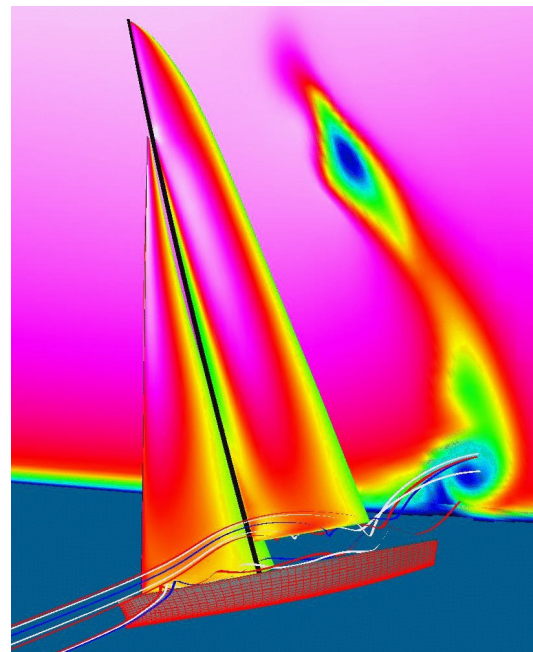


Figure 2: Typical Flow Visualization

A second example of this capability is demonstrated in Figure 3. It shows the difference between surface streamlines on the windward side of a high camber mainsail (left) and a low camber mainsail (right). The patterns are interpreted by noting that concentrations of streamlines are either separation lines or reattachment lines. If streamlines emerge from a concentration, the line is a reattachment line. Figure 3 shows one such line on each sail, and all flow upstream of these lines is therefore separated.

Since the two Genoas are identical, their separation patterns are similar, and remain limited to the upper half of the luff. This feature is often evident on high pointing boats where the higher telltails point upwards even when the sail is properly trimmed. Mainsail draft, however, has a significant effect on mast separation. The full sail at left has a much larger separation bubble than the flat sail on the right. This will cause lowered performance over that portion of the luff that contains the bubble.

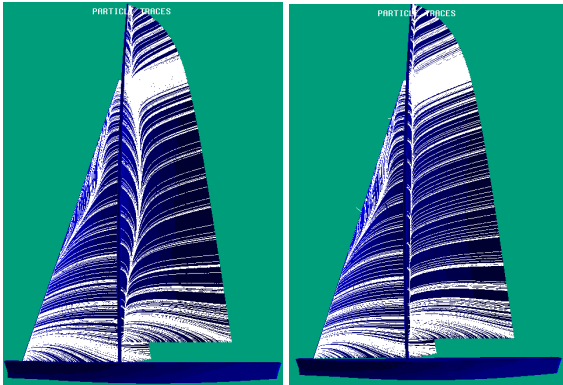


Figure 3: Comparison of Separation versus Camber

RANS is also useful for looking at one off design modifications. It is both faster and cheaper, for example, to prototype a new concept in the computer than on the water. A wide range of design concepts can be investigated with few resources, and only those that show merit need be built and tested. Figure 4 shows an example of how AmericaOne used this capability to investigate the viability of staysail combinations for upwind legs.

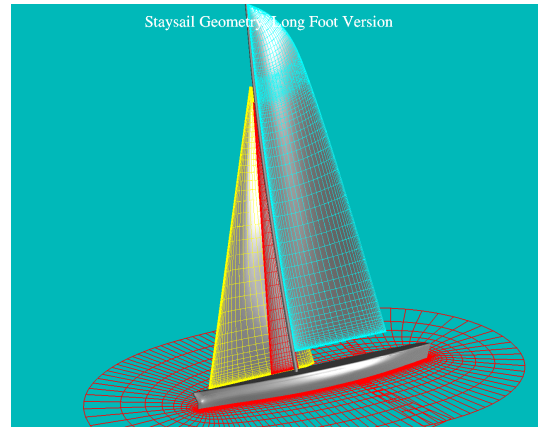


Figure 4: Numerical Prototype of Staysail Combination

Further qualitative examples are shown in figures 5 and 6. These figures depict two separate studies of sail shape design. Figures 5, represents the actual design shape while figure 6, represents the flying shape. The subtle difference in the delta Cp of the genoa and main sails can be seen when comparing the two figures. Figure 6, appears to have a smaller lobe of delta Cp positioned further forward on the sail, indicating a change in the camber distribution of the sail and the delta Cp. Upon further analysis, the actual force and moment centers shift due to the relaxed geometries. The understanding of the centers of the moment and forces has been a contributing factor to the design of the hull.

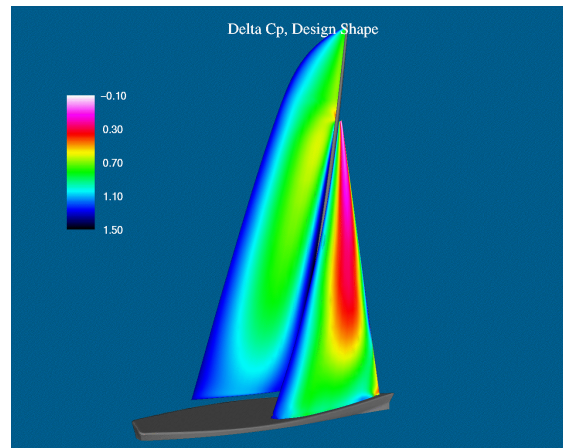


Figure 5: Design Shape

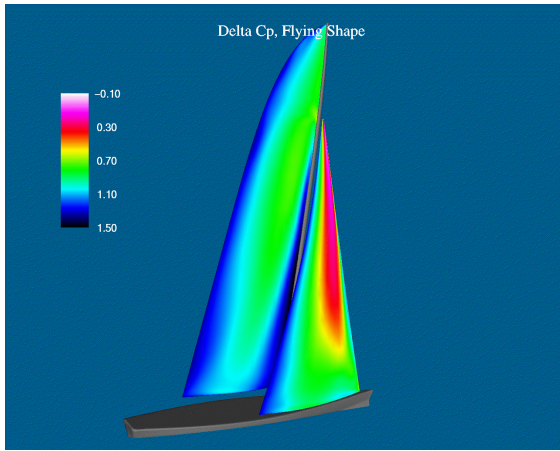


Figure 6: Flying Shape

DESIGN TRADE-OFF RESULTS

The use of RANS for quantitative ranking of designs covered a wide range of studies. A partial list of the studies performed includes:

- Sail camber variations
- Vertical camber distributions
- Horizontal camber variations
- Sail twist variations
- Mast section design
- Mast rake effects
- Mast structural deflection effects
- Sheeting angle variations
- Staysail comparisons
- Flying shape effects (i.e. relaxed geometries)
- Wind angle variations
- Mainsail roach and Genoa J variations
- Cockpit shape studies
- Standing rigging drag reduction
- Viscous corrections for VPP sail force predictions

The total effort for these studies covered more than two years and 360 three-dimensional RANS studies. The calculations created approximately 50 GigaBytes of data, and required significant reduction efforts before yielding practical input to the dozens of supported design studies.

One of the original motivations for introducing RANS into the design process was to quantify viscous effects on the choice of sail camber. Panel codes typically predict that sail lift-to-drag ratios will continue to increase as camber increases. It is well known, however, that a full sail creates more form drag, and that the lift-to-drag ratio will eventually decrease. Panel codes are deficient in that they cannot predict this

form drag, and RANS codes are required to prevent misleading trends.

Figures 7 and 8 depict the results of a RANS study that highlights these differences. The figures compare sail combinations of different camber, and show drag predictions from both panel and RANS predictions (drive force being the negative of drag). Figure 7 shows Genoa drive force versus wind angle, and indicates a startling result. The panel code predicts the second sail has more drive than the first whereas RANS predicts the opposite. Figure 8 shows total drag versus wind angle for the same two sails. Even though the trend is not reversed, RANS predicts a far greater advantage for one combination. It is also interesting to note that even though the study covers only a very small wind angle range, RANS predicts a nonlinear lift behavior whereas the panel codes do not.

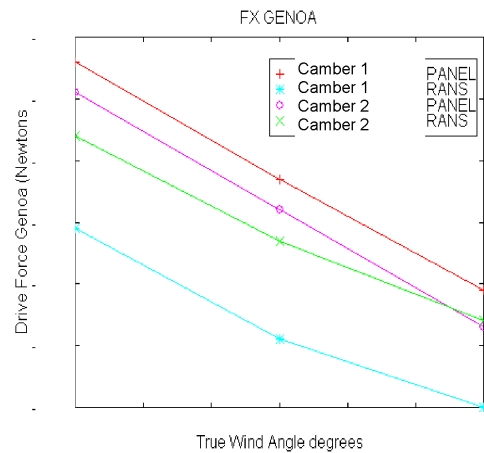


Figure 7: Genoa Drive Force Comparison

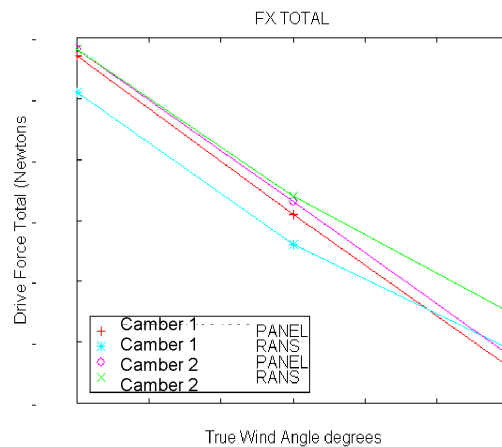


Figure 8: Total Drive Force Comparison

Despite the proven deficiencies of panel codes, they are still required for the majority of design work. Even with overset gridding, RANS is not sufficiently efficient to populate a VPP aerodynamic force database. This requires thousands of simulations, and must be

performed using panel codes. An important step in the design process, therefore, is to use RANS for correcting the panel-generated aero force database.

Figure 9 demonstrates one way RANS might be used to perform such a function. The results show ratios of force predicted from one numerical method to the force predicted from the other. The ratios depend on height above the deck, and are therefore plotted versus a vertical coordinate. Although they are also demonstrated to depend on camber, they can be used to approximately correct panel-generated aero force data bases to more RANS-like distributions.

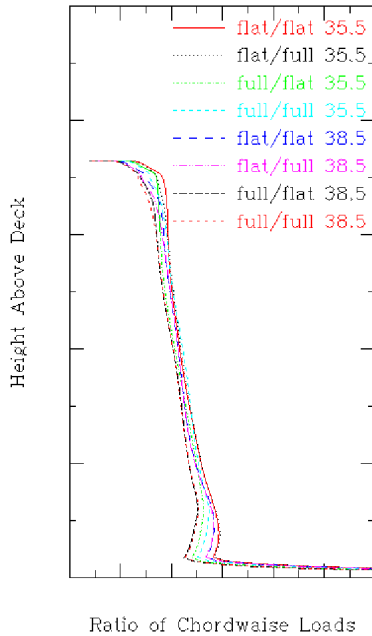


Figure 9: RANS/Panel Comparison

Another example of how RANS was used for quantifying design trends was in the study of mast shape. This included many aspects of mast design, from section profile, to rake, to deformation under load.

Figure 10 shows a typical study involving section shape. Each section has one curve, and drag is plotted versus vertical height up the mast. Curve elements towards the right side of the figure indicate “draggy” sections whereas curve sections towards the left indicate “driving” sections. Three of the four section shapes exhibit approximately equal drag while the fourth shows a 15 percent increase at the lower heights. This trend changes drastically at the top of the mast, where all four sections exhibit different drive force distributions.

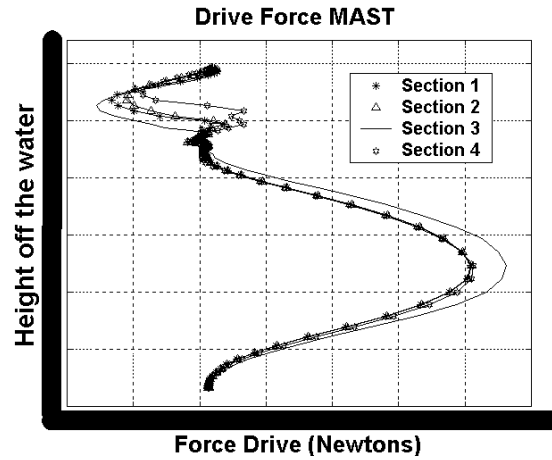


Figure 10: Mast Sectional Shape Comparison

Figures 11 through 13 show the detailed flow around 3 varying mast section shapes. Each image shows the flow in a plane formed by taking a cut perpendicular to the mast at a height above the hounds. Moving from Figure 11 to 13, the separation behind the mast on the leeward side is shown to be dependent on the mast shape. Depending on the design function, the section shape is crucial. An increased mast sectional shape may allow the designer to support a larger main sail roach, however this may come at a cost of drag. At the end of the day, RANS allows the designer the ability to trade off the function of sectional shape, mainsail roach and drag.

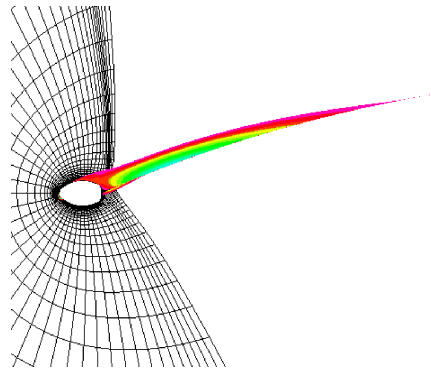


Figure 11: Flow Visualization (Section 1)

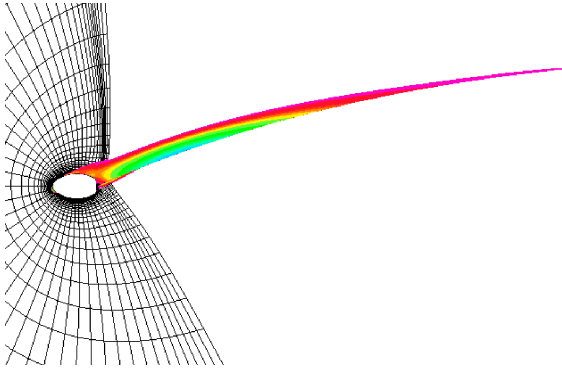


Figure 12: Flow Visualization (Section 2)

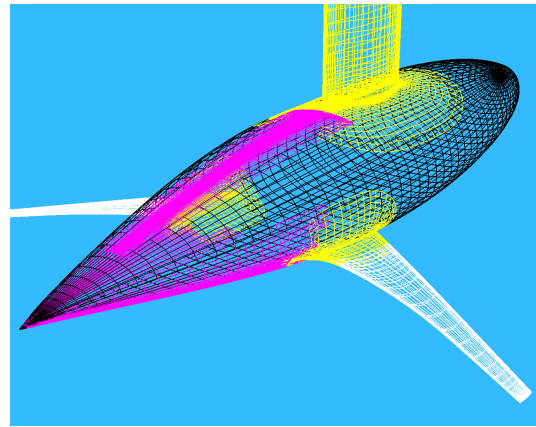


Figure 14: Typical Keel Grid

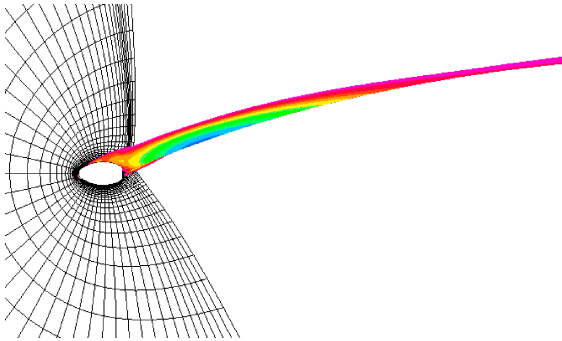


Figure 13: Flow Visualization (Section 3)

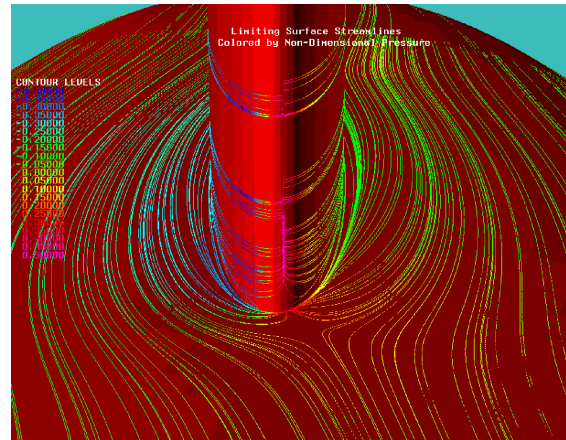


Figure 15: Surface Streamlines

KEEL/BULB/WINGLEY RESULTS

The use of RANS during America Cup XXX was not limited to sail design. The authors (along with others on the AmericaOne design team) also used RANS to analyze a number of candidate keel designs. Figure 14 shows an example of a typical keel grid. As the studies were intended to aid the winglet alignment process, all grids were designed to resolve the winglets, the bulb, and particularly the winglet/bulb interaction. Although the hull could have been included, it was typically represented as a flat plate. The runs were conducted at various speeds and yaw angles, and analyzed to insure proper winglet loading.

Figure 15 shows surface streamlines from a representative solution. The view looks aft towards the keel/bulb intersection at its leading edge, and the streamlines are colored by non-dimensional pressure. The keel angle of attack (leeway angle) is clearly evident, and the creation of a juncture vortex (due to the lack of a fillet in this case) is indicated by the saddle point and associated reattachment streamlines.

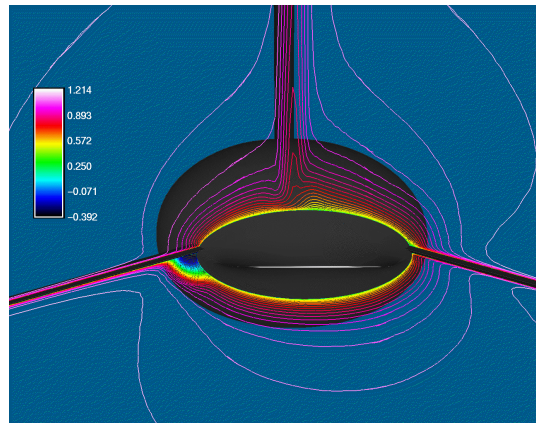


Figure 16: Streamwise Velocity in Transverse Plane

Figure 16 shows the bulb and winglet flow in a transverse plane taken near the winglet trailing edge. The case depicts a boat on starboard tack, with the high pressure side of the keel fin being to port. The associated keel-tip vortex will therefore be in the counter-clockwise direction (looking forward), and the winglets will capture a counter-clockwise lift. This causes the bottom of the port-side winglet to be the low pressure side, and makes for a weak boundary layer.

When combined with the weak boundary layer of the bulb closure, the wingley boundary layer can no longer sustain, and separates near its root. The separation pattern on the wingley underside is detailed by the surface streamlines of figure 17.

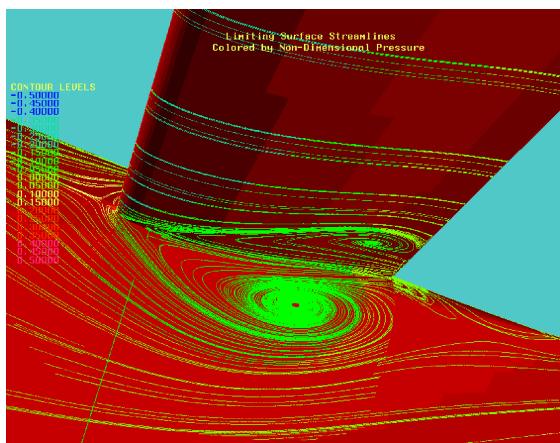


Figure 17: Streamlines (Under Windward Winglet)

CONCLUSIONS

The inclusion of viscous flow CFD in the IACC yacht design process is an essential element of a complete design process. RANS codes in particular have demonstrated their ability to incorporate viscous trending effects into hydrodynamic and aerodynamic yacht design. While RANS codes (like panel codes and experiments) still have their limitations, their applicability need not be limited as long as these limitations are well understood.

Americas Cup XXX demonstrated that RANS can be effectively integrated into the design loop. RANS was utilized to provide improved force and moment calculations (as compared to panel codes), and to accurately trend even subtle design details such as mast shape, sail camber, and winglet placement. Finally, RANS has been shown to provide sufficient flow field detail for guiding the process of design improvement.

The demonstrated use of RANS is just the beginning. Limitations imposed by computer speed and memory become less restrictive every year, and turnaround time can only continue to improve. RANS can therefore be expected to play a more significant role in Americas Cups to follow.

REFERENCES

Chen, H.C., and Korpus, R.A., 1993, "A Multi-Block Finite-Analytic Reynolds-Averaged Navier-Stokes method for 3-D Incompressible Flows." *ASME J. of Fluids Engineering*.

Chen, H.C., and Patel, V.C., 1988, "Near-Wall Turbulence Models for Complex Flows Including Separation," *AIAA Journal*, Vol. 26, No. 4, pp. 641-648.

Chen, H.c., and Patel, V.C., 1989, "The Flow Around Wing-

Body Junctions," *Proceedings, 4th Symposium on Num. And Phys. Aspects of Aerodynamic Flows*, Long Beach, CA.

Chen, H.C., Patel, V.C., and Ju, S., 1990, "Solutions of Reynolds-Averaged Navier-Stokes Equations for Three-Dimensional Incompressible Flows," *J. of Computational Physics*, Vol. 88, No.2, pp. 305-336.

Hanjalic,K., and Launder, B.E., 1980, "Sensitizing the Dissipation Equation to Irrotational Strains," *ASME J. of Fluids Engineering*, Vol. 102.

Korpus,R., 1995, "Six Years of Progress Under the ARPA SUBTECH Program," SAIC Report No. 95/1143.

Korpus,R., and Falzarano, J.M., 1997, " Prediction of Viscous Ship Roll Damping by Unsteady Navier-Stokes Techniques," *J. of Offshore Mech. and Arctic Eng.*, vol. 119, no 2., pp. 108-113.

Korpus,R., Jones,P., Oakley,O., Imas,L., 2000, "Prediction of Viscous Forces on Oscillating Cylinders by Reynolds-Averaged Navier-Stokes Solver," *The 11th International Society of Offshore and Polar Engineering Conference & Exhibition (ISOPE-2000)*, Seattle, WA.

Korpus,R., Hubbard,B., Jones,P., Stromgen,C., Bennett,J., 1998, "Hydrodynamic Design of Integrated Propulsor/Stern Concepts by Reynolds-Averaged Navier-Stokes Techniques," *Seventh International Symposium on Practical Design of Ship and Mobile Units (PRADS)*, The Hague, Netherlands.

Kumarasamy,S. Korpus,R., Barlow,J. 1997 "Computation of Noise Due to the Flow Over A Circular Cylinder," *Proceedings, 2nd Computational Aeroacoustics (CAA), Workshop on Benchmark Problems*, Tallahassee, Fl.

Weems, K., and Korpus, R., et al., 1994, "Near-Field Flow Predictions for Ship Design," *Proceedings, 20th Symposium Naval Hydrodynamics*, Santa Barbara, CA.